



# Computational Fluid Dynamic Simulation of Dispersed Oil-Water Flow with New Drop Coalescence Model

A. A. Amooey<sup>†</sup> and E. Omidbakhsh Amiri

*Department of Chemical Engineering, University of Mazandaran, Babolsar, Iran*

<sup>†</sup>Corresponding Author Email: [aliakbar\\_amooey@yahoo.com](mailto:aliakbar_amooey@yahoo.com)

(Received February 18, 2018; accepted August 10, 2018)

## ABSTRACT

The three-dimensional oil-water flow in horizontal pipe has been investigated by introducing population balance equation (PBE). The water fraction of inlet flow and mixture velocity varies from 46% to 60% and from 1.25 m/s to 3 m/s, respectively. The multiple size groups model has been applied to the non-uniform drop size distribution in oil-water flow. The drop coalescence models have a clear efficacy on the prediction capability of the PBE. In this work, drop coalescence model for oil-water is modified and used for predicting the phase distribution of dispersed oil - water in horizontal pipe. Population balance with modified Coualaloglou's frequency model is used. The attention of the modification is on the presence of droplets that reduce the free space for droplet motion and cause an enhancement in the collision frequency. The phase distribution profile from numerical results is presented and discussed. Acceptable agreement with the experimental data is achieved by using the modified coalescence model. Also, at 46% water fraction and mixture velocity equal as 3 m/s, model with population balance with modified Coualaloglou is 4% and 1% better than Luo's model and Coualaloglou's model, respectively.

**Keywords:** Drop coalescence; Population balance; Multiphase flow; Modeling.

## NOMENCLATURE

$B^B$	birth due to break-up of drops	$g$	gravity
$B^C$	birth due to coalescence of drops	$G$	generation of turbulent kinetic energy
$C_f$	increase coefficient of surface	$h$	film thickness
$C_D$	drag coefficient	$h_{ij}$	collision frequency
$C_L$	lift coefficient	$k$	turbulent kinetic energy
$C_{TD}$	turbulent dispersion	$k_c$	turbulent kinetic energy of continues phase per unit of mass
C13	constant of eq. (8)	$n_i$	drop number density
C14	constant of eq. (9)	$p$	pressure
$C_1$	constant order unity of eq. (10)	$R_d$	film radius
$C_{1\epsilon}$	constant of standard $k-\epsilon$ model	Re	Reynolds number
$C_{2\epsilon}$	constant of standard $k-\epsilon$ model	$t_{ij}$	time required for two drops to coalesce
$C_\mu$	constant of standard $k-\epsilon$ model	$S_{ij}$	the collision-sectional area
$\sigma_k$	constant of standard $k-\epsilon$ model	$S_i$	source term
$\sigma_\epsilon$	constant of standard $k-\epsilon$ model	$u$	velocity
$d$	diameter	$u_x$	x-component of velocity
$d_{32}$	Sauter mean bubble diameter	$u_{e1}$	velocity of eddy with size $d_1$
$D^B$	death due to break-up of drops	$u_{rel}$	approach velocity
$D^C$	death due to coalescence of drops	$V_i$	corresponding volume of a drop of group $i$
$f_i$	volume fraction of drops of a group $i$	We	Weber number
$f_{BV}$	breakage volume fraction	$y$	normal distance
$F_{cd}$	sum of the interfacial forces	$\alpha$	volume fraction
$F_D$	drag force	$\epsilon$	rate of energy dissipation per unit of liquid mass
$F_L$	lift force	$\mu$	dynamic viscosity
$F_{TD}$	turbulent force		

$\zeta$	size ratio between an eddy and a particle
$\nu$	kinetic viscosity
$\rho$	density
$\sigma$	surface tension
$\tau_{ij}$	contact time for two drops
$\tau_k$	shear stress tensor
$\chi_{ij}$	coalescence rate
$\Omega(V_j, V_i)$	break-up rate of drops of volume $V_j$
$\lambda'$	modified factor for collision frequency

#### subscript

c	continuous phase
d	dispersed phase
o	oil
w	water (or wall)
l,tur	liquid phase, turbulent flow
$\alpha$ ,tur	turbulent flow
$\alpha$ ,lam	laminar flow
$\alpha$ ,eff	effective
mix	mixture

## 1. INTRODUCTION

The study of breakup and coalescence particle is important topic in industrial applications. The nuclear reactor, condensation and boiling equipment which ones are as multiphase flow are case studies of this application.

The population-balance-equation (PBE) model has been usually applied in the recently years (Valentas and Amundson, 1996; Hounslow and Ni, 2004; Raikar *et al.*, 2009; Qin and Chen, 2016). This model explains the background of a drop population with some properties such as drop coalescence, breakage. Some randomly events which has been distributed in time can be adopted by the PBE model. The coalescence of two drops is often performed in three stages contains colliding drop, draining liquid layer and drop coalesce.

Dispersed two-phase oil-water flows are encountered in many industrial applications. In dispersed flow one phase is present in the form of droplets, in a continuous carrier phase and different droplet size distributions may occur according to the flow condition. An example of dispersed flow is the petroleum industry, where oil and water are produced simultaneously from reservoirs. The prediction of hold-up and pressure gradient in two-phase dispersed flow has been investigated for several years (Gao *et al.*, 2003).

Experimental study of pressure drop at high velocity and volume fraction are difficult (Madhavan, 2005). In very few literatures, detail explanations of numerical studies have been reported for dispersed liquid-liquid flows (Moe, 1993). With one dimensional tool, the liquid content, pressure drop and flow regimes were studied (Lun *et al.*, 1996). In their models, the flow regimes, liquid fraction between phases and wall friction were studied. Two and three dimension two-phase flow had been studied by Moe (1993) and Bendiksen *et al.* (1991) by the use of semi-implicit finite difference scheme. Computational Fluid Dynamic (CFD) is useful tools for optimization of process and equipment design in industrial oil. The simulation results of two-phase dispersed flow in a horizontal pipe are much infrequent in available literature (walvekar *et al.*, 2009; Seaton *et al.*, 2011 Pouraria *et al.*, 2013; Picchi *et al.*, 2015).

One of effective design parameter for multiphase

flow is hold-up of phase. This parameter illustrates the concentration of dispersed phase in mixture. The hold-up influences the drop pressure and many transport processes. Also, this parameter is able to introduce the total residence time of the dispersed phase.

Solving the present gap (i.e., the simulation outcomes of dispersed oil-water) in the literature is the main focus, here. In this work, a combination of population balance (with three Coalescence model) with computational fluid dynamics (CFD) has been implemented for the case of distribution oil-water in horizontal pipe. This work compared Luo *et al.* (1993) and Coualaloglou *et al.* (1977) coalescence models. Also, in this work, Coualaloglou *et al.* (1977) model was modified. In this modification, the existence of droplets which was Reducing the free space due to droplet movement and lead to increasing of collision frequency, has been evaluated. Then, it compared with these two coalescence models. The results of the models were compared with experimental data.

## 2. NUMERICAL MODELING

### 2.1 Mass Conservation Equation

Eulerian-Eulerian two-fluid model was used in these numerical simulations (Drew and Passman, 1988). These equations can be written as Equations (1) and (2) for continuous and dispersed phases:

$$\frac{\partial(\rho_c \alpha_c)}{\partial t} + \nabla \cdot (\rho_c \alpha_c u_c) = 0 \quad (1)$$

$$\frac{\partial(\rho_d \alpha_d f_i)}{\partial t} + \nabla \cdot (\rho_d \alpha_d u_d f_i) = S_i \quad (2)$$

where  $c$  indicates continuous phase (water),  $d$  indicates dispersed phase (oil),  $f_i = \alpha_{di} / \alpha_i$  and  $S_i$  is a source term which is included the birth and death of drops caused by coalescence and break up processes (Equation (3)). For the drop with constant and uniform size, it is clear that  $S_i = 0$ .

$$S_i = B_i^B + B_i^C - D_i^B - D_i^C \quad (3)$$

where  $i$  changes from 1 to  $N$  and  $B^B, B^C, D^B$  and  $D^C$  are respectively defined as ‘birth’ and ‘death’ due to break-up and coalescence of drops and can be written as below:

$$\begin{aligned}
B_i^B &= \sum_{j=i+1}^N \Omega(V_j, V_i) n_j \\
B_i^C &= 0.5 \sum_{k=1}^N \sum_{j=1}^N \chi_{ij} n_i n_j \\
D_i^B &= \Omega_i n_i \\
D_i^C &= \sum_{j=1}^N \chi_{ij}
\end{aligned} \quad (4)$$

The drop number density  $n_i$  is related to dispersed-phase volume fraction ( $\alpha_d$ ) by  $\alpha_d f_i = n_i V_i$  where  $V_i$  is volume of a drop of group  $i$ . The break-up rate of drops of volume  $V_j$  ( $= V f_{BV}$ ) can be obtained as Luo' work (1996).

### 2.1.1 Model Development

With oscillation turbulent velocity of the circumambient liquid, bubbles or drops may be colliding each other. It is commonly assumed that the random movement of fluid particles in a turbulent flow behaves like a random motion of gas molecules in the theory of gas- kinetics theory. However, the fluid particles are neither rigid nor elastic. Based on the kinetic gas theory of Kennard (1938), the collision frequency can be explained as:

$$h(d_i, d_j) = S_{ij} u_{rel} \quad (5)$$

where  $S_{ij}$  is the collision-sectional area of colliding droplets, and can be written as

$$S_{ij} = \frac{\pi(d_i + d_j)^2}{4} \quad (6)$$

For calculating of the approach velocity  $u_{rel}$ , it is often presumed that the colliding drop/bubble take the velocity of equalized eddy (Luo, 1993; Coualaloglou and Tavlarides (1977). Because of inadequate energy of a small eddy, bubble/drop does not motion, while, the larger eddies just move bubbles/drops and have no other effect on the relative motion. So, the relative velocity between two bubbles/drops of size  $d_i$  and  $d_j$  is written as:

$$u_{rel} = (u_{ii}^2 + u_{jj}^2)^{1/2} \quad (7)$$

Where  $u_{i1}$  is the velocity of eddy with size  $d_1$ .

Although, for the computing of eddy velocity  $u_t$ , the inertial sub range of isotropic turbulent is usually presumed. With classical turbulent theories, it can be said

$$u_t^2 = C_{13} (\varepsilon_c d)^{2/3} \quad (8)$$

Then, the collision frequency can be indicated as Luo, 1993)

$$h_{ij} = \frac{C_{14} \pi (d_i + d_j)^2 (d_i^{2/3} + d_j^{2/3})^{1/2} \varepsilon_c^{1/3}}{4} \quad (9)$$

The coalescence rate with turbulent collision from Luo (1993) can be written as

$$\begin{aligned}
\chi_{ij} &= \left(\frac{\pi}{4}\right) (d_i + d_j)^2 (u_{ii}^2 + u_{jj}^2)^{1/2} \\
&\exp \left\{ -\frac{c_1 \left[ (0.75(1 + x_{ij}^2)(1 + x_{ij}^3))^{1/2} \right]}{[(\rho_d / \rho_c + 0.5)^{1/2} (1 + x_{ij}^3)] We_{ij}^{1/2}} \right\}
\end{aligned} \quad (10)$$

where  $C_1$  is a constant order unity,  $x_{ij} = d_i / d_j$ , Weber number is defined as

$$We_{ij} = \frac{\rho_c d_i (u_{ii}^2 + u_{jj}^2)}{\sigma} \quad (11)$$

The turbulent velocity  $u_t$  (Rotta, 1974) is:

$$u_t = 1.4 \varepsilon_c^{1/3} d^{1/3} \quad (12)$$

And another coalescence rate as for turbulent collision from Coualaloglou and Tavlarides (1977) can be written as

$$\begin{aligned}
\chi_{ij} &= 1.37 \varepsilon_c^{1/3} (d_i^{2/3} + d_j^{2/3})^{1/2} \\
&(d_i^2 + d_j^2) \exp \left( \frac{-t_{ij}}{\tau_{ij}} \right)
\end{aligned} \quad (13)$$

where  $\tau_{ij}$  is contact time for two drops specified with  $(d_{ij}/2)^{2/3} \varepsilon_c^{1/3}$  and  $d_{ij}$  is equivalent diameter that Chesters and Hoffman (1982) suggested as

$$d_{ij} = \left( \frac{2}{d_i} + \frac{2}{d_j} \right)^{-1} \quad (14)$$

$t_{ij}$  is time required for two drops, with diameter of  $d_i$  and  $d_j$  to coalesce is estimated as

$$\begin{aligned}
t_{ij} &= 0.5 \mu_c R_d^2 \left\{ \begin{aligned} & -2 \ln \left[ h_{crit} + \left( \frac{k_2}{k_1} \right)^{1/3} \right] + \ln \left[ h_{crit}^2 - h_{crit} \left( \frac{k_2}{k_1} \right)^{1/3} + \left( \frac{k_2}{k_1} \right)^{2/3} \right] \\ & + 2\sqrt{3} \arctan \left[ \frac{1}{3} \frac{[-2h_{crit} + \left( \frac{k_2}{k_1} \right)^{1/3}] \sqrt{3}}{\left( \frac{k_2}{k_1} \right)^{1/3}} \right] \\ & + 2 \ln \left[ h_{int} + \left( \frac{k_2}{k_1} \right)^{1/3} \right] - \ln \left[ h_{int}^2 - h_{int} \left( \frac{k_2}{k_1} \right)^{1/3} + \left( \frac{k_2}{k_1} \right)^{2/3} \right] \\ & - 2\sqrt{3} \arctan \left[ \frac{1}{3} \frac{[-2h_{int} + \left( \frac{k_2}{k_1} \right)^{1/3}] \sqrt{3}}{\left( \frac{k_2}{k_1} \right)^{1/3}} \right] \end{aligned} \right\} / k_1 \left( \frac{k_2}{k_1} \right)^{2/3}
\end{aligned} \quad (15)$$

The parameter  $h_{int}$  and  $h_{crit}$  illustrate the film thickness when collision begins and critical film at which rupture caused respectively.  $R_d$  is film radius and  $k_1 = 4\sigma(d_i + d_j)/(d_i d_j)$  and  $k_2 = 2.335 \times 10^{-20}$ .

In Eq. (13) an effect is not considered: this is the reduction of the free space for droplet motion due to the volume occupied by droplets. So we proposed collision frequency as follow:

$$\chi_{ij} = 1.37 \varepsilon_c^{1/3} (d_i^{2/3} + d_j^{2/3})^{1/2} (d_i^2 + d_j^2) \exp\left(\frac{-\tau_{ij}}{\tau_{ij}}\right) \lambda' \quad (16)$$

The presence of droplets that reduce the free space for droplet motion and cause an enhancement in the collision frequency, is the main subject in modification view. This effect can be considered by multiplying the collision frequency with a factor  $\lambda'$  where  $\lambda' = 1/(1-\alpha_d)$ ,  $\alpha_d$  denotes the volume fraction of the droplets. The  $\lambda'$  term in equation (16) reflects the limited range of the turbulent fluctuations affecting the motion of the droplets.

## 2.2. Momentum Equations

The momentum conservation for multiphase flow is explained as follow:

$$\frac{\partial(\rho_c \alpha_c u_c)}{\partial t} + \nabla \cdot (\rho_c \alpha_c u_c u_c) = -\alpha_c \nabla p + \quad (17)$$

$$\rho_c \alpha_c g - \nabla(\alpha_c \tau_c) + F_{cd}$$

where  $u$  is the volume averaged velocity and  $\tau_k$  is the phase shear stress tensor,  $F_{km}$  demonstrates the sum of the interfacial forces that include the drag force  $F_D$ , lift force  $F_L$  and turbulent force ( $F_{TD}$ ). The drag and lift forces are obtained as (Tomiyama *et al.*, 2002):

$$F_D = \left(\frac{3}{4}\right) C_D \alpha_d \rho_c \left(\frac{1}{d_{32}}\right) |\bar{u}_c - \bar{u}_d| (\bar{u}_c - \bar{u}_d) \quad (18)$$

$$F_L^c = -F_L^d = C_L \alpha_d \rho_c (\bar{u}_d - \bar{u}_c) \times \nabla \times \bar{u}_c \quad (19)$$

where  $|\bar{u}_c - \bar{u}_d|$  is the slip velocity,  $d_{32}$  is the disperse phase Sauter mean bubble diameter,  $C_L$  is the lift coefficient (In this study  $C_L = -0.05$ ),  $C_D$  is drag coefficient and is written as (Kumar and Hartland, 1985):

$$C_D = \left(0.53 + \frac{24}{Re}\right) \times (1 + 4.56 \alpha_d^{0.73}) \quad (20)$$

The turbulent dispersion force, from Lopez de Bertodano's work (1992) approximates as turbulent diffusion of drops by the contentious eddies. It is expressed as:

$$F_{TD}^c = -F_{TD}^d = -C_{TD} \rho_c k_c \nabla \alpha_c \quad (21)$$

where  $k_c$  is the liquid turbulent kinetic energy per unit of mass and  $C_{TD}$  is the turbulent dispersion coefficient. In this Study, turbulent dispersion coefficient of Simonin and Viollet (1990) has been used for simulation (*i.e.*,  $C_{TD} = 7.5$ ).

## 2.3 Turbulence Models

In here, the standard  $k-\varepsilon$  model proposed by Launder and Spalding (Launder and Spalding, 1972) is applied. The governing equations for the turbulent kinetic energy  $k$  and turbulent dissipation

$\varepsilon$  are:

$$\frac{\partial(\rho_c \alpha_c k)}{\partial t} + \frac{\partial(\rho_c \alpha_c u_c k)}{\partial x_i} =$$

$$\frac{\partial}{\partial x_i} \left( \alpha_c \left( \mu_c + \frac{\mu_{i,tur}}{\sigma_k} \right) \frac{\partial k}{\partial x} \right) + \alpha_c (G - \alpha_c \rho_c \varepsilon_c) \quad (22)$$

$$\frac{\partial(\rho_c \alpha_c \varepsilon_c)}{\partial t} + \frac{\partial(\rho_c \alpha_c u_c \varepsilon_c)}{\partial x_i} =$$

$$\frac{\partial}{\partial x_i} \left( \alpha_c \left( \mu_c + \frac{\mu_{i,tur}}{\sigma_\varepsilon} \right) \frac{\partial \varepsilon_c}{\partial x_i} \right)$$

$$+ \alpha_c \left( \frac{\varepsilon_c}{k} \right) (C_{1\varepsilon} G - C_{2\varepsilon} \alpha_c \rho_c \varepsilon_c) \quad (23)$$

where  $C_{1\varepsilon}$ ,  $C_{2\varepsilon}$ ,  $C_\mu$ ,  $\sigma_k$  and  $\sigma_\varepsilon$  are standard  $k-\varepsilon$  model constant (Launder and Spalding, 1972). The turbulent viscosity of the continuous phase is calculated by

$$\mu_{\alpha,tur} = \frac{C_\mu \rho_c k_c^2}{\varepsilon_c} \quad (24)$$

The effective viscosity can be written as

$$\mu_{\alpha,eff} = \mu_{\alpha,lam} + \frac{\mu_{\alpha,tur}}{\sigma_k} \quad (25)$$

## 2.4 Boundary conditions

At the inlet, the uniform actual velocity of inlet flow was defined in all the simulations.

$$u_x = 0 \quad u_y = 0 \quad u_{z,d} = \frac{u_{mix}}{1 + (\alpha_d / \alpha_c)}$$

$$u_{z,d} = u_{z,c} \left( \frac{\alpha_d}{\alpha_c} \right) \quad (26)$$

Where the  $\alpha$  is volume fraction of phase. The velocity for each phase was calculated. The dispersed phase from Soleimani's work (1999) was used. Pressure outlet boundary conditions was accounted for outlet. The atmosphere pressure was specified at outlet. 'No-slip' boundary condition was applied at wall. Schematic of model with boundary conditions are shown in Fig. 1.

$$u_x = 0 \quad u_y = 0 \quad u_z = 0 \quad (27)$$

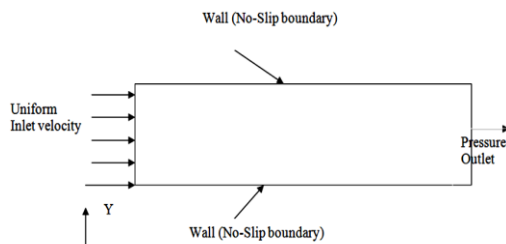


Fig. 1. Boundary conditions of this work.

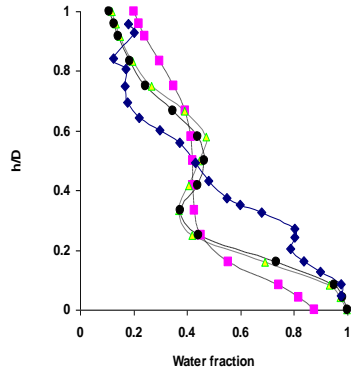


Fig. 2.  $h/D$  versus water fraction with 46% of water in inlet (velocity of mixture is 1.25 m/s):  $\blacklozenge$ - Experimental;  $\blacksquare$ -CFD with PBE (Luo);  $\blacktriangle$ - CFD with PBE (Coulaloglou);  $\bullet$ - CFD with PBE (modified Coulaloglou).

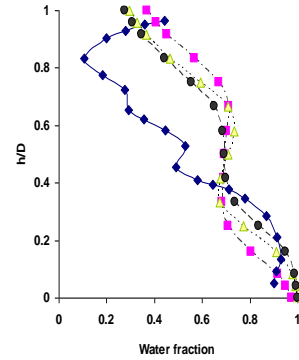


Fig. 4.  $h/D$  versus water fraction with 60% of water in inlet (velocity of mixture is 1.25 m/s):  $\blacklozenge$ - Experimental;  $\blacksquare$ -CFD with PBE (Luo);  $\blacktriangle$ - CFD with PBE (Coulaloglou);  $\bullet$ - CFD with PBE (modified Coulaloglou).

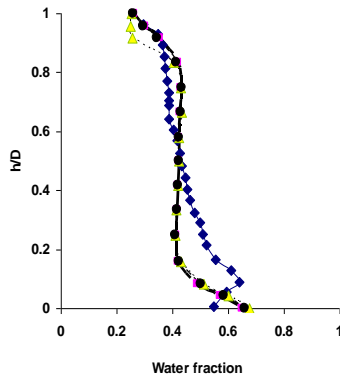


Fig. 3.  $h/D$  versus water fraction with 46% of water in inlet (velocity of mixture is 2.12 m/s):  $\blacklozenge$ - Experimental;  $\blacksquare$ -CFD with PBE (Luo);  $\blacktriangle$ - CFD with PBE (Coulaloglou);  $\bullet$ - CFD with PBE (modified Coulaloglou).

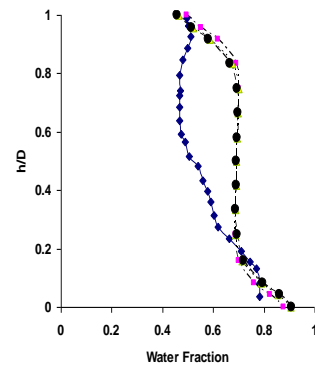


Fig. 5.  $h/D$  versus water fraction with 60% of water in inlet (velocity of mixture is 2.12 m/s):  $\blacklozenge$ - Experimental;  $\blacksquare$ -CFD with PBE (Luo);  $\blacktriangle$ - CFD with PBE (Coulaloglou);  $\bullet$ - CFD with PBE (modified Coulaloglou).

### 3. NUMERICAL SOLUTION PROCEDURE

In this work, 3-D transient flow in a horizontal pipe 24.  $\times$  9700 mm ( $r \times z$ ) using the commercial software FLUENT (Version 6.3) which is based on an Eulerian-Eulerian scheme, were simulated. For creating of non-uniform grid with 'quadrilateral' cells, GAMBIT software was used. The unsteady solver was applied to solve on all grids. The first order upwind scheme was applied to discretize the convective terms. Water and oil were considered as the continuous and dispersed phases, respectively. In this work, drop ranging from 0.1 to 0.5 mm diameter divided in to 8 classes (according  $V_{i+1} = 2V_i$ ). The Multiple Size Group (MUSIG) model (Lo, 1996) has been used in FLUENT (Version 6.3) to account for the non-uniform drop size distribution in oil-water dispersed flow. A supplementary set of eight transport equations were solved for tracking of the discrete drop sizes assigned in the dispersed phase. These

equations with the flow equations were employed during the simulations. In general, there are eight different complete phases, but in this work, for reducing the computational resource and time, it was considered that each drop class tracked at the same mean algebraic velocity. So, eight equations of continuity for dispersed phase with one continuity equation for the continuous phase were coupled with each other. The time step is 0.005 s. Under-relaxed factors are between 0.7 and 0.8, except for pressure which one is equal to 0.3. The semi-implicit method for the pressure linked equation (SIMPLE) scheme was utilized for solving pressure-velocity decoupling. Absolute convergence criteria is  $10^{-4}$  in this work.

### 4. RESULTS AND DISCUSSION

The density and viscosity of oil are 801  $kg/m^3$  and 1.6 cP, respectively. The water fraction at inlet changes between 46% and 60%. Also, The mixture velocity varies from 1.25 m/s to 3m/s. In two locations, results are considered: at near outlet of

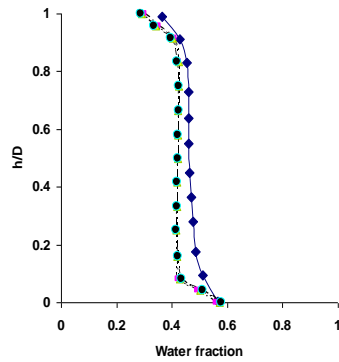


**Fig. 6.**  $h/D$  versus water fraction with 46% of water in inlet (velocity of mixture is 3 m/s): ♦- Experimental; ■-CFD with PBE (Luo); ▲- CFD with PBE (Coulaloglou); ●- CFD with PBE (modified Coulaloglou).

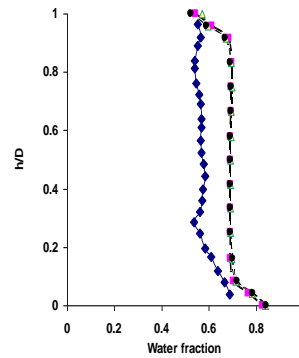


**Fig. 8.**  $h/D$  versus water fraction with 60% of water in inlet (velocity of mixture is 3 m/s): ♦- Experimental; ■-CFD with PBE (Luo); ▲- CFD with PBE (Coulaloglou); ●- CFD with PBE (modified Coulaloglou).

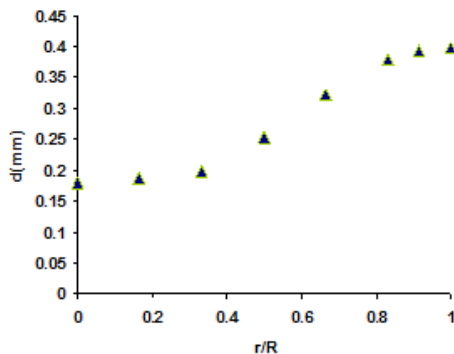


**Fig. 7.** Sauter mean drop diameter at vertical position, At mixture velocity 2.12 and volume fraction 46%.

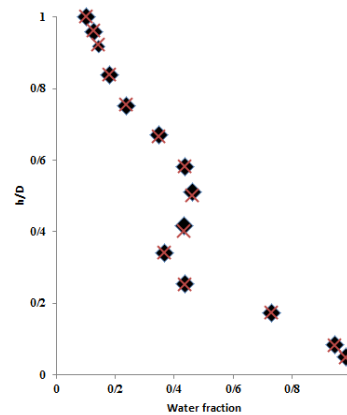


**Fig. 9.**  $h/D$  versus water fraction with 46% of water in inlet (velocity of mixture is 1.25 m/s), (CFD with PBE (modified Coulaloglou)); ♦ 452330 node; × 947282 node.

pipe and a vertical line passing the center of the pipe axis. Also in this work, we defined subroutine for coalescence model and drag coefficient in the FLUENT software.

Figs.2-7 show variations of the  $h/D$  for water fraction of 46% and 60% at inlet and for mixture velocity of 1.25m/s, 2.12m/s and 3 m/s, respectively. The predicted CFD combination PBE with three Coalescence model (Luo (1993), Coulaloglou (1977) and modified Coulaloglou (1977)) results is compared with experimental data of Soleimani (1999). The results of simulation of phase shows accommodation with the experimental data at lower water fraction and high mixture velocities. The results of the model show better agreement with the experimental data with population balance with modified Coulaloglou (1977). As, at lower water fraction and higher mixture velocity, the difference between experimental data and model with population balance with modified Coulaloglou (1977) is almost 10%.

A decrease in drop size from wall to center of pipe in Fig. 8 is seen due to increase in phase velocity. At bottom and top of pipe, the hold-up could be

predicted with CFD simulation. However, there is a difference between experimental and present CFD simulations when the water fraction at inlet was increased from 46% to 60%. At the bottom of pipe cross section and 60% input water, it can be found a fair agreement with experimental data.

Two drop coalescence model are tested. Quantitative agreements between the experimental data and simulation are obtained. The results show that Luo (1993) coalescence model, Coulaloglou (1977) coalescence model and modified model coalescence for mixture velocity 1.25 m/s 2.12 m/s and 3 m/s give good quantitative agreement with the experimental data, but modified model coalescence model give better corresponding with results than Luo (1993) coalescence model and Coulaloglou(1977) coalescence model.

It can be observed from that the CFD simulation with modified Coulaloglou (1977) (Figs. 2, 3) that at the top of pipe where volume fraction oil phase increase coalescence increase so volume fraction water shift to left and at bottom pipe, the oil phase decreases, the coalescence decreases so volume fraction water shift to Right.

Simulations with different numbers of node (such as 452330, 947282) was done. Fig.9 shows there is no clear difference between these two dispersed volume fraction profiles. It can be seen that dispersion due to turbulence is the highest near to the wall, thus droplets tend to move out of wall and stay longer in the core region where turbulence is lower. Also lift force is important in the boundary layer and pushes the droplets towards the core zone.

As, at 46% water fraction and mixture velocity equal as 3 m/s, model with population balance with modified Coualoglou is 4% and 1% better than Luo's (1993) model and Coualoglou's (1977) model, respectively. Although, for 60% water fraction and mixture velocity equal as 1.25 m/s, model with population balance with modified Coualoglou is 26% and 8% better than Luo's (1993) model and Coualoglou's (1977) model, respectively.

It can be observed from the CFD simulation that when mixing velocity increases from 1.25 to 3 m/s, the water fraction profile increases and flats, thus liquid layer shrinks. At oil and water velocity of 3 m/s, are uniformly and oil fraction is homogeny at pipe.

The CFD results using population balance could also predict acceptably well the hold-up at top and bottom of the pipe. As illustrated in Figs. 2-7 the oil droplets are focused around the center and the upper section of the pipe so an annular zone of relatively high water fraction founds around this oil-rich core. These results accommodate qualitatively with Ward and Knudsen's (1967) results.

## 5. CONCLUSION

A CFD model has been simulated for oil-water dispersed flow in horizontal pipe. The phase hold-up from numerical result is presented and discussed. Acceptable accommodation with the experimental data is achieved with three coalescence of population balance model for wide range mixture velocity. The modified coalescence model prediction shows better accommodation with the experimental data. As, at lower water fraction and higher mixture velocity, the difference between experimental data and model with population balance with modified Coualoglou is almost 10%. Model with population balance with modified Coualoglou is better than Luo's and Coualoglou's model. At higher mixture velocity, the predicted phase distribution was in good agreement while disagreement was be seen for lower mixture velocity.

## REFERENCES

Bendiksen, K., D. Maines, R. Moe and S. Nuland (1991). The dynamic two-fluid model OLGA: Theory and Application. *Society of Petroleum Engineers*. 6 (2), 171-180.

Chesters, A. K. and G. Hoffman (1982). Bubble coalescence in pure liquids. *Applied Scientific*

*Research*. 38, 353-361.

Coulaloglou, C. A. and L. L. Tavlarides (1977). Description of Interaction Processes in Agitated Liquid-Liquid Dispersions. *Chemical Engineering Science*. 32 (11), 1289-1297.

Drew, D. A. and S. L. Passman (1988) Theory of Multicomponent Fluids. Springer-Verlag, USA.

FLUENT User Guide. (2006) <http://www.Fluent.Inc/fluent6.3>

Gao, H., H. Y. Gu and L. J. Guo (2003). Numerical study on stratified oil-water two phase turbulent flow in horizontal tube. *International Journal of Heat Mass transfer*. 46, 749-754.

Hounslow, M. J. and X. Ni (2004). Population balance modelling of droplet coalescence and break-up in an oscillatory baffled reactor. *Chemical Engineering Science*. 59(4), 819-828.

Kennard, E. H. (1938). *Kinetic Theory of Gases*. McGraw-Hill, New York.

Kumar, A. and S. Hartland (1985) Gravity settling in liquid-liquid dispersions. *The Canadian Journal of Chemical Engineering*. 63, 368-376.

Lauder, B. E. and D. B. Spalding (1972). *Mathematical Models of Turbulence*. Academic Press, London.

Lo, S. (1996). *Application of the MUSIC model to bubbly flows*. AEAT-1096, AEAT Technology.

Lopez de Bertodano, M. A. (1992). Turbulent bubbly two-phase flow in a triangular duct. Ph.D. Dissertation, Rensselaer Polytechnic Institute, Troy, New York .

Lun, I., R. K. Calay and A. E. Holdo (1996). Modeling two-phase flow using CFD. *Journal of Applied Energy*. 53, 299-314.

Luo, H. (1993). Coalescence, breakup and liquid circulation in bubble column reactors. Ph.D. thesis, Trondheim, Norway.

Luo, H. and H. F. Svendsen (1996). Theoretical model for drop and bubble break-up in turbulent dispersions. *AIChE Journal*. 42, 1225-1233.

Madhavan, S. (2005). CFD Simulation of Immiscible Liquid Dispersions. M.Sc Thesis, Dalhousie University, Canada.

Moe, R. (1993). Transient simulation of 2-3D stratified and intermittent 2-phase flows. *International Journal for Numerical Methods in Fluids*. 16, 461-487.

Picchi, D., D. Strazza, M. Demori, V. Ferrari and P. Poesio (2015). An experimental investigation and two-fluid model validation for dilute viscous oil in water dispersed pipe flow. *Experimental Thermal and Fluid Science*. 60, 28-34.

- Pouraria, H., J.K. Paik and J.K. Seo (2013). Modeling of two-phase oil/water flow in horizontal pipeline using CFD technique. *Proceedings of the International Conference on Offshore Mechanics and Arctic Engineering*, Nantes, France.
- Qin, C. and C. Chen (2016). CFD-PBM simulation of droplets size distribution in rotor-stator mixing devices. *Chemical Engineering Science* 155, 16-26.
- Raikar, N. B., S.R. Bhatia, M. Malone and A. Henson (2009). Experimental studies and population balance equation models for breakage prediction of emulsion drop size distributions. *Chemical Engineering Science* 64 (10), 2433-2447.
- Rotta, J. C. (1974). *Turbulence Stromungen*, Stuttgart, Germany.
- Seaton, M.A., I. Halliday, and A. J. Masters (2011), Application of the multicomponent lattice Boltzmann simulation method to oil/water dispersions. *Journal of Physics A: Mathematical and Theoretical* 44(10), Article number 105502.
- Simonin, O. and P. Viollet (1990). Predictions of an oxygen droplet pulverization in compressible subsonic co flowing hydrogen flow. *Numerical Methods for Multiphase Flows*. 91, 65-82.
- Soleimani, A. (1999) Phase distribution and associated phenomena in oil-water flows in horizontal tube, Ph.D. Thesis, Imperial College, London.
- Tomiyama, A., H. Tamai, I. Zun and S. Hosokawa (2002). Transverse migration of single bubbles in simple shear flows. *Chemical Engineering Science*. 57 (11), 1849-1859.
- Valentas, K. J. and N. R. Amundson (1996). Breakage and Coalescence in Dispersed Phase Systems. *Industrial and Engineering Chemistry Fundamentals*. 5, 533-542.
- Walvekar, R. G., T. S. Y. Choong, S. A. Hussain, M. Khalid and T.G. Chuah (2009). Numerical study of dispersed oil-water turbulent flow in horizontal tube, *Journal of Petroleum Science and Engineering* 65 (3-4), 123-128.
- Ward, J. P. and J. G. Knudsen (1967). Turbulent Flow of Unstable Liquid-Liquid Dispersion: Drop Sizes and Velocity Distributions. *AIChE journal*. 13(2), 356-362.